Published in final edited form as:
Biochem Pharmacol. 2012 June 15; 83(12): 1643–1654. doi:10.1016/j.bcp.2012.03.010.

Mitochondrial Superoxide Mediates Doxorubicin-Induced Keratinocyte Apoptosis through Oxidative Modification of ERK and Bcl-2 Ubiquitination

Sudjit Luanpitpong[a,b], **Pithi Chanvorachote**[b], **Ubonthip Nimmannit**[c], **Stephen S. Leonard**[d], **Christian Stehlik**[e], **Liying Wang**[d], and **Yon Rojanasakul**[a,*]

[a]Department of Pharmaceutical Sciences,West Virginia University, Morgantown, WV 26506, USA [b]Faculty of Pharmaceutical Sciences, Chulalongkorn University, Bangkok 10330, Thailand [c]National Nanotechnology Center, National Science and Technology Development Agency, Pathumthani 12120, Thailand [d]Pathology and Physiology Research Branch, National Institute for Occupational Safety and Health, Morgantown, WV 26506, USA [e]Department of Medicine, Northwestern University, Chicago, IL 60611, USA

Abstract

Massive apoptosis of keratinocytes has been implicated in the pathogenesis of chemotherapy-induced skin toxicities, but the underlying mechanisms of action are not well understood. The present study investigated the apoptotic effect of doxorubicin (DOX) on HaCaT keratinocytes and determined the underlying mechanisms. Treatment of the cells with DOX induced reactive oxygen species (ROS) generation and a concomitant increase in apoptotic cell death through the mitochondrial death pathway independent of p53. Electron spin resonance and flow cytometry studies showed that superoxide is the primary oxidative species induced by DOX and responsible for the death inducing effect. Ectopic expression of mitochondrial superoxide scavenging enzyme (MnSOD) or treatment with MnSOD mimetic (MnTBAP) inhibited DOX-induced superoxide generation and apoptosis. The mechanism by which superoxide mediates the apoptotic effect of DOX was shown to involve downregulation of Bcl-2 through ubiquitin-proteasomal degradation. Superoxide induces dephosphorylation of Bcl-2 through MAP kinase ERK1/2 inactivation which promotes ubiquitination of Bcl-2. We also provide evidence for the oxidative modification of ERK1/2 through cysteine sulfenic acid formation. These findings indicate a novel pathway for redox regulation of apoptosis regulatory proteins which could be important in the understanding of chemotherapy-induced toxicities and development of preventive treatment strategies which are currently lacking.

Keywords

Apoptosis; doxorubicin; keratinocytes; reactive oxygen species; ERK; Bcl-2

[*]**Corresponding author** West Virginia University Department of Pharmaceutical Sciences P.O. Box 9530, Morgantown, WV 26506. Phone: +1 304 293 1476 FAX : +1 304 293 2576 yrojan@hsc.wvu.edu.

Disclosure The authors have no conflict of interest to disclose.

1. Introduction

Doxorubicin (DOX) is the mainstay chemotherapeutic agent against various hematological malignancies and solid tumors, including breast cancer, lung cancer and sarcoma, but with limited cumulative doses [1,2]. Numerous side effects have been reported in patients undergoing DOX treatment, including skin toxicities such as alopecia and skin ulcerations, myelosuppression and myopathy [1,3-5]. Alopecia or massive hair loss is arguably the most feared and most common side effect of chemotherapy. In addition, occupational cutaneous exposure to DOX has been reported [6,7]. Accumulating evidence indicate that uncontrolled apoptosis plays a key role in skin toxicities of DOX [8,9]. Apoptosis is a tightly regulated process and is executed along two major pathways (extrinsic and intrinsic) [10,11]. The extrinsic pathway involves death receptor activation and induction of death signaling complex leading to apoptosis, while the intrinsic pathway involves the release of cytochrome *c* from the mitochondria which binds to caspase-activating proteins such as Apaf-1 and activates the caspase cascade [12]. Bcl-2 is a key regulator of the intrinsic pathway by interfering with the release of cytochrome *c* or its binding to Apaf-1 through its interaction with Bax [13,14]. Thus, downregulation of Bcl-2 by DOX provides a key mechanism of apoptosis induction by the agent.

DOX has been shown to induce reactive oxygen species (ROS) generation in various cell types, which has been linked to its action [15-17]. Mitochondria are the major source of ROS generation and are involved in apoptotic cell death induced by various stimuli [18,19]. The role of ROS in Bcl-2 regulation has been reported to occur primarily through ubiquitin-proteasomal degradation [20,21], but the underlying mechanism and specific ROS involved have not been demonstrated. Dephosphorylation of Bcl-2 is an essential step for Bcl-2 ubiquitination [21,22]. One of the major phosphorylation-dephosphorylation signaling cascades is mitogen-activated protein (MAP) kinases, including p44/p42 extracellular signal-related kinases (ERK1/2), c-Jun-N-terminal protein kinase (JNKs), and p38 kinase [23,24]. We hypothesized that one or more of these kinases is responsible for the dephosphorylation and ubiquitination of Bcl-2 in response to DOX treatment.

The overall objective of this study was to identify the specific ROS involved and determine the underlying mechanisms of DOX-induced skin toxicities. We identified mitochondrial superoxide as a key mediator of DOX-induced apoptosis and discovered an oxidative protein modification process via cysteine sulfenic acids as a potential regulator of ERK signaling and DOX-induced apoptosis. This novel finding could have a major implication in the regulation of redox-sensitive proteins under oxidative stress conditions. Human keratinocytes were tested in this study since they are the primary target for DOX-induced toxicities. HaCaT keratinocytes, although exhibited alterations in their life-span (immortalizion), were used as they express typical epidermal phenotype [25-27], of which making them common *in vitro* models to aid the mechanistic studies of skin and hair follicle [28,29].

2. Materials and Methods

2.1. Cell culture

Human keratinocyte HaCaT cells were obtained from Cell Lines Service (Heidelberg, Germany) and maintained in Dulbecco's modified Eagle's medium (DMEM) (Gibco, Gaithersburg, MA) supplemented with 10% fetal bovine serum, 2 mM L-glutamine, 100 units/ml of penicillin and 100 μg/ml of streptomycin in 5% CO_2 at 37°C.

2.2. Reagents

Doxorubicin, Mn(III)tetrakis(4-benzoic acid) porphyrin chloride (MnTBAP) and concanamycin A were obtained from EMD Biosciences (La Jolla, CA). *N*-acetyl cysteine (NAC), cell permeable catalase (catalase-polyethylene glycol; CAT), dimethylthiourea (DMTU), lactacystin, and antibody for ubiquitin were obtained from Sigma Chemical (St. Louis, MO). Hoechst 33342, di-hydrodichlorofluorescein diacetate (H_2DCF-DA), dihydroethidium (DHE), and Mitosox™ were obtained from Molecular Probes (Eugene, OR). Caspase inhibitor benzyloxycarbonyl-Val-Ala-Asp(OMe) fluoromethylketone (zVAD-fmk), caspase-8 inhibitor benzyloxycarbonyl-Ile-Glu(OMe)-Thr-Asp(OMe)-fluoromethylketone (zIETD-fmk), and caspase-9 inhibitor benzyloxycarbonyl-Leu-Glu(OMe)-His-Asp(OMe)-fluoromethylketone (zLEHD-fmk) were from Alexis Biochemicals (San Diego, CA). Antibody for Bcl-2, phospho-Bcl-2 (serine 87), and protein G-conjugated agarose were from Santa Cruz Biotechnology (Santa Cruz, CA). Antibodies for Bax, MAP kinases and phospho-MAP kinases ERK1/2, SAPK/JNK, p38, β-actin, and peroxidase-conjugated secondary antibodies were from Cell Signaling Technology (Boston, MA). PD98059 (MAP kinase ERK1/2 inhibitor), SP600165 (c-Jun N-terminal kinase inhibitor), and SB203580 (p38 MAP kinase inhibitor) were from Calbiochem (La Jolla, CA). Antibody for cysteine sulfenic acid was from Millipore (Billerica, MA).

2.3. Plasmids and transfection

Manganese superoxide dismutase (MnSOD) plasmid was generously provided by Dr. X. Shi (University of Kentucky, School of Medicine, Lexington, KY). Authenticity of the plasmid construct was verified by DNA sequencing. HaCaT cells were transfected with MnSOD or pcDNA3 control plasmid by nucleofection using Amexa Biosystems Nucleofector (Cologne, Germany), according to the manufacturer's instructions. Cells were suspended in 100 μl of nucleofection solution with 2 μg of plasmid and nucleofected using the device program U020. The cells were resuspended in 500 μl of complete medium and seeded in 6-mm cell culture dish, after which they were allowed to recover for 72 h before each experiment. Transfection efficiency was determined by using a GFP reporter plasmid and was found to be approximately 85%.

2.4. Apoptosis assays

Apoptosis was determined by Hoechst 33342 and caspase activation assays. In the Hoechst assay, cells were incubated with 10 μg/ml of Hoechst 33342 for 30 min and analyzed for apoptosis by scoring the percentage of cells having intensely condensed chromatin and/or fragmented nuclei by fluorescence microscopy (Leica Microsystems, Bannockburn, IL). Approximately 1,000 nuclei from ten random fields were analyzed for each sample. The apoptotic index was calculated as the percentage of cells with apoptotic nuclei over total number of cells.

2.5. Caspase activity assays

Caspase activity was determined by using APO LOGIX carboxyfluorescein caspase detection kit (Cell Technology, Minneapolis, MN), according to the manufacturer's instructions. After specific treatments, cells were incubated with 10 μl of 30x FAM-DEVD-fmk, FAM-LETD-fmk, or FAM-LEHD-fmk for 2 h in dark for caspase-3, -8, or -9 activity determinations respectively. The cells were washed with 1x Working Dilution Wash buffer which was supplied with the kit. The fluorescence signals were measured using a fluorescence microplate reader (FLUOstar, BMG Labtech, Durham, NC) at the excitation and emission wavelengths of 488 and 520 nm, respectively. Caspase activity was expressed as the ratio of fluorescence signal from the treated and control samples.

2.6. ROS detection

ROS generation was measured by flow cytometry and by electron spin resonance (ESR). The former utilizes dichlorodihydrofluorescein diacetate (H_2DCF-DA) as a general oxidative probe and dihydroethidium (DHE) as a superoxide anion probe, whereas the latter uses 5,5-dimethyl-1-pyrroline-*N*-oxide (DMPO) as a spin trapper. For flow cytometric measurements, cells were incubated with the probe (10 μM) for 30 min at 37°C, after which they were washed and resuspended in phosphate buffered saline (PBS) and immediately analyzed for dichlorofluorescein (DCF) intensity using a 485-nm excitation beam and 538-nm band-pass filter, or dihydroethidium (DHE) intensity using a 488-nm excitation beam and a 610-nm band-pass filter (FACSort, Becton Dickinson, Rutherford, NJ). Mean fluorescence intensity was quantified by CellQuest software (Becton Dickinson) analysis of the recorded histograms. For ESR measurements, cells were incubated with the spin trapper DMPO (10 mM) for 10 min at 37°C in the presence or absence of specific ROS scavengers to aid characterization of the generated free radicals. The ESR signals were measured using a Bruker EMX spectrometer (Bruker Instruments, Billerica, MA) and a flat cell assembly. Hyperfine couplings were measured (to 0.1 G) directly from magnetic field separation using potassium tetraperoxochromate and 1,1-diphenyl-2-picrylhydrazyl as reference standards. An Acquisit program (Bruker Instruments) was used for data acquisition and analysis.

2.7. Mitochondrial superoxide detection

Mitochondrial superoxide formation was detected by fluorescence microscopy using MitoSOX™ Red as a specific fluorescent probe. Briefly, cells were incubated with 5 μM of the probe for 30 min at 37°C in dark. They were then washed thoroughly with warm HBSS buffer and mounted for imaging. MitoSOX™ Red was visualized using an excitation wavelength of 546 nm and an emitter band pass of 605 nm.

2.8. Western blot analysis

After specific treatments, cells were incubated with lysis buffer containing 20 mM Tris-HCl (pH 7.5), 1% Triton X-100, 150 mM sodium chloride, 10% glycerol, 1 mM sodium orthovanadate, 50 mM sodium fluoride, 100 mM phenylmethyl-sulfonyl fluoride, and a commercial protease inhibitor mixture (Roche Molecular Biochemicals) at 4°C for 20 min. Cell lysates were collected and determined for protein content using the Bradford method (Bio-Rad Laboratories, Hercules, CA). Proteins (40 μg) were resolved under denaturing conditions by 10% sodium dodecyl sulfate-polyacrylamide gel electrophoresis (SDS-PAGE) and transferred onto nitrocellulose membranes The transferred membranes were blocked for 1 h in 5% nonfat dry milk in TBST (25 mM Tris-HCl, 125 mM NaCl, 0.05% Tween-20) and incubated with appropriate primary antibodies at 4°C overnight. The membranes were washed twice with TBST for 10 min and incubated with horseradish peroxidase-conjugated secondary antibodies for 1 h at room temperature. The immune complexes were then detected by chemiluminescence detection system (Amersham Biosciences, Piscataway, NJ) and quantified using Analyst/PC densitometry software (Bio-Rad Laboratories, Hercules, CA).

2.9. Immunoprecipitation

After specific treatments, cells were washed with PBS and lysed in lysis buffer at 4°C for 20 min. The lysates were collected and determined for protein content using the Bradford method (Bio-Rad Laboratories). Cell lysates (60 μg protein) were incubated with anti-Bcl-2 or anti-ERK1/2 (p44/p42) antibody at 4°C for 14 h, followed by incubation with protein G-conjugated agarose for 4 h at 4°C. The immune complexes were washed 6 times with cold lysis buffer and resuspended in 2x Laemmli sample buffer. The immune complexes were separated by 10% SDS-PAGE and analyzed by Western blotting as described.

2.10. Cysteine sulfenic acid detection

Cells were washed with PBS and lysed in lysis buffer containing 0.1 mM dimedone 4°C for 20 min. Cell lysates (60 μg protein) were immunoprecipitated and separated by 10% SDS-PAGE as described. Cysteine sulfenic acid was detected by Western blotting using 1:1000 anti-cysteine sulfenic acid antibody (Millipore) and anti-rabbit horseradish peroxidase-conjugated secondary antibody. Quantification was performed using Analyst/PC densitometry software.

2.11. Statistical analysis

The data represent means ± S.D. from three or more independent experiments. Statistical analysis was performed by Student's t test at a significance level of $p < 0.05$.

3. Results

3.1. Doxorubicin induces apoptosis of HaCaT cells through mitochondrial death pathway

To characterize the apoptosis response to DOX treatment in human keratinocytes, HaCaT cells were treated with various concentrations of DOX (0-3 μM) and apoptosis was determined after 24 h by Hoechst 33342 assay. DOX treatment caused a dose-dependent increase in apoptosis, the effect that was inhibited by co-treatment of the cells with pan-caspase inhibitor zVAD-fmk or antioxidant *N*-acetyl cysteine (NAC) (Fig. 1A). The apoptotic cells exhibited condensed or fragmented nuclei with intense nuclear fluorescence (Fig. 1B). The inhibitory effect of NAC primarily suggested the role of ROS in the apoptosis induction by DOX, which is confirmed in subsequent studies using specific ROS scavengers. Figure 1C shows that DOX induced caspase-3 activation in a dose-dependent manner in concomitant with the observed nuclear morphological changes, supporting caspase-dependent apoptosis of the cells by DOX. Caspase-9 inhibitor (zLEHD-fmk) effectively inhibited the caspase-3 activation of DOX, whereas caspase-8 inhibitor (z-IETD-fmk) was ineffective. Because caspase-9 serves as the apical caspase of the intrinsic (mitochondrial) death pathway and caspase-8 represents the apical caspase of the extrinsic pathway [12,14], these results suggest mitochondrial death pathway as a major pathway of apoptosis induced by DOX. The requirement of mitochondrial death pathway was confirmed by the observation that DOX markedly induced caspase-9 activation, whereas it had no significant effect on caspase-8 activity (Fig. 1D).

3.2. Doxorubicin induces ROS generation in HaCaT cells

To determine whether DOX induces ROS generation in HaCaT cells, cellular ROS levels in the cells after DOX treatment were measured by flow cytometry using H_2DCF-DA as a fluorescent probe. H_2DCF-DA is a general oxidative probe that can detect multiple ROS. Figure 2A shows that DOX was able to increase ROS fluorescence intensity which was inhibited by the addition of antioxidant NAC. To further investigate the specific ROS generated, cells were treated with DOX in the presence or absence of various specific ROS scavengers, including catalase (hydrogen peroxide scavenger), MnTBAP (MnSOD mimetic and superoxide scavenger), and DMTU (hydroxyl radical scavenger). Cellular ROS generation was then determined by flow cytometry as earlier described. Figure 2B shows that co-treatment of the cells with MnTBAP, but not with catalase or DMTU, completely inhibited the ROS-inducing effect of DOX, suggesting superoxide as the primary oxidative species produced by cells in response to DOX treatment.

To confirm ROS generation in the treated cells, ESR measurements were performed using DMPO as a spin trapping agent. The ESR technique was used because it allows more accurate identification of the specific ROS involved. The hyperfine coupling of spin adduct is generally characteristic of the original trapped radical. In this study, cells were treated

with DOX in the presence or absence of specific ROS scavengers and analyzed for free radical generation. Non-treated cells with DMPO were used as a negative control. In the presence of added DOX, a clear positive signal was observed (Fig. 2C). Based on the line shape and hyperfine splitting, the spectrum observed is indicative of superoxide anion. To our knowledge, this is the first demonstration of the superoxide generation in DOX-treated cells detected by ESR. The identity of superoxide formation was confirmed by the observation that MnTBAP (superoxide scavenger), but not other ROS scavengers, inhibited the ESR signal (Fig. 2C). These results are consistent with the flow cytometric results and indicate superoxide as the major ROS induced by DOX in HaCaT cells.

3.3. Doxorubicin induces mitochondrial superoxide generation

The induction of superoxide by DOX was confirmed by flow cytometry using dihydroethidium (DHE) as a fluorescent probe. The result shows that DOX was able to increase cellular DHE fluorescence intensity in a dose-dependent manner (Fig. 3A). We also used mitochondria-targeted hydroethidium (MitoSOX™ Red) to investigate mitochondria as the potential source of superoxide generation. Figure 3B shows DOX-induced MitoSOX fluorescence intensity which was inhibited by MnTBAP, supporting the generation of mitochondrial superoxide induced by DOX.

3.4. Mitochondrial superoxide mediates doxorubicin-induced apoptosis

Having demonstrated DOX-induced superoxide generation and apoptosis in HaCaT cells, we next tested whether superoxide is a key mediator of apoptosis induced by DOX. Cells were treated with DOX in the presence or absence of MnTBAP and analyzed for apoptosis. As controls, cells were similarly treated DOX with or without catalase or DMTU to determine the specificity of inhibition. Figure 4A shows that MnTBAP but not catalase or DMTU inhibited the apoptosis induced by DOX. MnTBAP also inhibited DOX-induced caspase-9 activation, whereas catalase and DMTU were ineffective (Fig. 4B). To test the role of mitochondrial superoxide in the death signaling process, cells were ectopically transfected with mitochondrial SOD (MnSOD) or control plasmid, and their effect on DOX-induced apoptosis was examined. Western blot analysis of MnSOD-transfected cells showed an increase in MnSOD protein expression over vector-transfected control (Fig. 4C). The MnSOD overexpressing cells also exhibited substantially reduced apoptotic response to DOX treatment as compared to vector-control cells (Fig. 4C). Overexpression of MnSOD also caused a significant decrease in DOX-induced superoxide generation (Fig. 4D), supporting the role of mitochondrial superoxide in DOX-induced apoptosis.

3.5. Effect of doxorubicin treatment on apoptosis-regulatory proteins

The mitochondrial apoptosis pathway is regulated by the balance of pro- and anti-apoptotic proteins, particularly the Bcl-2 family proteins. We examined two key apoptosis-regulatory proteins in the Bcl-2 family, namely Bax and Bcl-2, and evaluated their response to DOX treatment. In addition, p53 and its active phosphorylated form were also examined. Immunoblot studies showed that DOX induced a downregulation of the anti-apoptotic Bcl-2 protein but caused an upregulation of the pro-apoptotic Bax protein (Fig. 5A). DOX surprisingly downregulated the pro-apoptotic p53 protein, but upregulated its phosphorylated form at low DOX doses. Since the expression of p53 and its active form showed no correlation with the apoptotic response, our results suggest that DOX-induced is independent of p53 but dependent on Bcl-2.

3.6. Doxorubicin regulates Bcl-2 and Bax through superoxide

To determine the role of superoxide in Bcl-2 and Bax regulation, the expression levels of Bcl-2 and Bax after DOX treatment were determined. To test the role of superoxide, cells

were treated with DOX in the presence or absence with MnTBAP, catalase or DMTU, and analyzed for Bcl-2 and Bax expression by Western blotting. In agreement with the apoptosis and caspase activation data (Fig. 4, A and B), DOX-induced downregulation of Bcl-2 was inhibited by MnTBAP, but not by catalase or DMTU (Fig. 5B). MnTBAP also inhibited the effect of DOX on Bax, whereas catalase and DMTU had no effect. Since the fate of cells is determined by the balance of pro- and anti-apoptotic proteins, the Bcl-2-to-Bax ratio was shown. Additionally, the role of ROS in p53 activation was determined since phosphorylation of p53 was detected. The results showed that none of the ROS scavengers had significant inhibitory effect on DOX-induced p53 phosphorylation (Fig. 5B), supporting the independence of p53 in the apoptotic process. Together, these results indicate the role of superoxide in Bcl-2 and Bax alterations and in apoptosis induced by DOX.

3.7. Doxorubicin induces Bcl-2 ubiquitination through superoxide

Bcl-2 has been shown to be regulated by ubiquitin-proteasomal degradation under diverse apoptotic conditions [20,21]. To determine whether this pathway is involved in the downregulation of Bcl-2 induced by DOX, cells were treated with DOX in the presence or absence of lactacystin, a specific proteasome inhibitor, and Bcl-2 expression was determined by Western blotting. As lysosomal degradation is another possible pathway of protein degradation, cells were also treated with DOX in the presence of lysosome inhibitor, concanamycin A, and analyzed for Bcl-2 expression. Figure 6A shows that lactacystin, but not concanamycin A, inhibited Bcl-2 downregulation induced by DOX, suggesting proteasomal degradation as the primary mechanism of Bcl-2 downregulation by DOX.

As proteasomal degradation is triggered by protein ubiquitination [30], we tested whether DOX could induce Bcl-2 ubiquitination in HaCaT cells. The cells were treated with DOX for various times and cell lysates were prepared and immunoprecipitated with anti-Bcl-2 antibody. The immune complex was then analyzed for ubiquitination using anti-ubiquitin antibody. The results show that DOX induced Bcl-2 ubiquitination as early as 1 h and peaked at approximately 2 h after the treatment (Fig. 6B). Treatment of the cells with MnTBAP completely inhibited the ubiquitination of Bcl-2 induced by DOX, whereas other ROS scavengers (catalase and DMTU) were unable to inhibit the ubiquitination (Fig. 6C). These results indicate that superoxide is the major oxidative species involved in the Bcl-2 ubiquitination.

3.8. Superoxide mediates dephosphorylation of Bcl-2 and ERK1/2 by doxorubicin

Ubiquitination of Bcl-2 has been reported to be dependent on its phosphorylation status [21,22], but the underlying mechanism is unclear. Certain apoptotic agents such as lipopolysaccharide and cisplatin have been shown to induce Bcl-2 dephosphorylation that triggers its ubiquitination and subsequent proteasomal degradation [21,31]. We tested whether DOX can induce Bcl-2 dephosphorylation and if so by what mechanism. Figure 7A shows that DOX treatment at 6 h did induce Bcl-2 dephosphorylation in a dose-dependent manner and that this effect occurred at the doses that induce apoptosis, superoxide generation, and Bcl-2 ubiquitination (1-3 μM). To investigate the mechanism of Bcl-2 dephosphorylation, we tested whether certain MAP kinases could act as Bcl-2 kinases. First, cells were treated with DOX and analyzed for various MAP kinase activities, including ERK1/2, JNK and p38 kinases. Figure 7A shows that DOX caused an inactivation (dephosphorylation) of ERK1/2 at the doses that induce Bcl-2 dephosphorylation, whereas it had an opposite effect (phosphorylation) on JNK1 and p38 kinases. JNK2 phosphorylation was also examined but was undetectable in the test cell system. These results suggest that ERK1/2, but not JNKs and p38 kinase, is the potential Bcl-2 kinase.

To verify the role of ERK1/2 in Bcl-2 dephosphorylation and ubiquitination, cells were treated with DOX in the presence or absence of MAP kinases inhibitors PD98059 (ERK1/2 inhibitor), SB203580 (p38 inhibitor) or SP600125 (JNK inhibitor), and their effects on Bcl-2 dephosphorylation and ubiquitination were determined. The results show that the ERK1/2 inhibitor PD98059 increased the dephosphorylation and ubiquitination of Bcl-2 by DOX, whereas the p38 inhibitor SB203580 had minimal effects (Fig. 7, B and C). The JNK inhibitor SP600125 promoted the Bcl-2 phosphorylation which can be attributed to its activation of ERK1/2 (Fig. 7B). MAP kinases inhibitors alone did not have profound effects on neither the phosphorylation of Bcl-2 nor cell apoptosis. Collectively, these results substantiate the role of ERK1/2 in Bcl-2 phosphorylation and its inactivation by DOX that contributes to Bcl-2 ubiquitination.

To further provide supporting evidence that ERK1/2 signaling acts upstream of Bcl-2 phosphorylation, time course measurement of the effect of DOX on phosphorylation of ERK and Bcl-2 were shown (Fig. 7D). While the ERK dephosphorylation was detected as early as 1 h and peaks at 3 h, Bcl-2 dephosphorylation, although was first observed at 1 h, has maximum response at 6 h, thus confirming that ERK1/2 is truly an upstream event.

Since Bcl-2 ubiquitination induced by DOX was shown to be dependent on ROS, we tested whether ROS might mediate its effect through ERK1/2 inactivation and Bcl-2 dephosphorylation. Cells were treated with DOX in the presence or absence of specific ROS scavengers including MnTBAP, catalase and DMTU, and ERK1/2 and Bcl-2 phosphorylation was determined. Figure 8A shows that treatment of the cells with MnTBAP, but not catalase or DMTU, completely inhibited DOX-induced ERK1/2 and Bcl-2 dephosphorylation. These results are consistent with the apoptosis and ubiquitination data and indicate that superoxide mediates the destabilizing effect on Bcl-2 by inactivating ERK1/2, leading to dephosphorylation and ubiquitin-proteasomal degradation of Bcl-2.

3.9. Superoxide induces ERK1/2 cysteine sulfenic acid formation

To provide a mechanistic insight to the mechanism of ERK1/2 inactivation by DOX, we investigated the possible oxidative modification of ERK1/2 by measuring cysteine sulfenic acid (Cys-SOH) formation. Cys-SOH generally serves as an oxidative regulator of protein function [32, 33], but its formation in ERK1/2 has not been demonstrated. To test this possibility, cells were treated with DOX and ERK1/2 was isolated by immunoprecipitation using anti-ERK1/2 antibody. The resulting immune complex was then probed for Cys-SOH formation using Cys-SOH specific antibody. Figure 8, B and C, shows that DOX treatment caused a dose-dependent increase in ERK1/2 Cys-SOH formation and that superoxide scavenger (MnTBAP) but not other scavengers (catalase and DMTU) inhibited such formation. These results are consistent with the role of superoxide as a key mediator of DOX-induced apoptosis through its ability to inactivate ERK1/2 and dephosphorylate Bcl-2 leading to ubiquitin-proteasomal degradation. The results also suggest that oxidative modification of ERK1/2 via Cys-SOH formation could be a key mechanism of apoptosis regulation in DOX-treated cells.

4. Discussion

DOX is a highly effective chemotherapeutic agent that is widely used to treat a variety of cancers. However, due to chemoresistance, the dosing of DOX has been increased causing serious side effects and compromising patient's quality of life [1,2,34]. Among the various side effects of DOX, alopecia and related skin toxicities are most common with no effective preventive treatment [5,35]. Increasing evidence indicate that excessive apoptosis of keratinocytes is largely responsible for the toxicities, but the underlying mechanisms are unclear. In this study, we demonstrated that DOX induced apoptosis of human keratinocytes

through the mitochondrial death pathway in association with caspase-9 activation (Fig. 1) and ROS generation (Fig. 2). Although DOX has been reported to induce ROS generation and apoptosis in various cell types, the identity of specific ROS involved in the toxicity and their cellular sources are unclear and controversial [16,36].

Using ESR and flow cytometry, we demonstrated that superoxide is the major oxidative species induced by DOX in HaCaT cells (Fig. 2). This notion is supported by the observations that the superoxide scavengers MnTBAP and MnSOD, but not other ROS scavengers (catalase and DMTU) inhibited the ROS generation induced by DOX (Figs. 2 and 4). We also found that mitochondria are the primary source of superoxide generation based on the observations that (i) mitochondrial SOD (MnSOD) and its mimetic (MnTBAP) were able to inhibit the superoxide generation, and (ii) the generated superoxide was detected by the mitochondrial ROS probe MitoSOX (Fig. 3). This finding is consistent with the established role of mitochondria as a key source of ROS production through the electron transport chain [10,18,19]. ROS are generated during the mitochondrial metabolic process primarily as superoxide that results from incomplete coupling of electrons, and depending on the expression of its scavenging enzymes determines the degree of subsequent ROS generation including hydrogen peroxide and hydroxyl radicals [37]. The relatively high level of superoxide in DOX-treated cells compared to hydrogen peroxide and hydroxyl radicals (Fig. 2) suggests the low abundance of MnSOD or the increased presence of catalase and other peroxide-scavenging enzymes in the cells.

The functional role of specific ROS in DOX-induced apoptosis was determined by co-treating the cells with ROS scavengers and analyzing apoptosis by caspase and nuclear fragmentation assays. Only superoxide scavengers (MnTBAP and MnSOD) were found to be effective in inhibiting the apoptosis, whereas other scavengers (catalase and DMTU) were ineffective (Fig. 4). These results are in good agreement with the ROS generation data (Fig. 2) and indicate that superoxide is the primary oxidative species and key mediator of DOX-induced apoptosis in the test cell system.

It is well documented that Bcl-2 family proteins play a major role in apoptosis regulation of the mitochondrial death pathway [10,11,38]. We found that DOX induced downregulation of Bcl-2 and upregulation of Bax in concomitant with caspase activation and apoptosis induction (Fig. 5). The superoxide scavenger MnTBAP inhibited these effects, whereas other ROS scavengers had no or minimal effects, substantiating the role of superoxide in the death signaling process. Since p53 was reported to regulate Bcl-2 family proteins through transcription-dependent and - independent mechanisms [39] and others have reported the induction of p53 activation and apoptosis by DOX in other cell systems [16,40], we tested whether p53 activation is responsible for DOX-induced apoptosis in HaCaT cells. Our results indicate that although p53 is activated (phosphorylated) by the DOX treatment, such activation is not required or functionally linked to the apoptotic effect. This conclusion is based on the observations that (i) DOX did not induce p53 activation at high doses (Fig. 5) where it induced extensive apoptosis, and (ii) superoxide scavenger MnTBAP effectively inhibited DOX-induced apoptosis but had no inhibitory effect on p53 (Fig. 5). Together, our results indicate that DOX-induced apoptosis in HaCaT cells is mediated through p53 independent but Bcl-2 dependent mechanisms.

The anti-apoptotic function of Bcl-2 is closely associated with its expression level which is controlled by various mechanisms depending on the apoptotic stimuli [20-22]. Our results indicate that DOX-induced downregulation of Bcl-2 is mediated through superoxide-dependent ubiquitin-proteasomal degradation (Fig. 6). The mechanism by which superoxide induces Bcl-2 ubiquitination involves dephosphorylation of the protein via MAP kinase ERK1/2 pathway (Fig. 7). DOX inactivates this pathway, the effect that can be prevented by

superoxide scavenging but not other ROS scavenging (Fig. 8), further confirming the role of superoxide in the death signaling process. This finding has not been reported elsewhere and could be important in the development of novel preventive treatment strategies that reduce the toxic side effects of DOX.

We have also demonstrated that ROS, particularly superoxide, have a structural altering effect on ERK1/2 protein by inducing Cys-SOH formation (Fig. 8). To the best of our knowledge, this is the first demonstration of the direct oxidative modification of ERK1/2 which could be important in its functional control under oxidative stress conditions. It is plausible that Cys-SOH formation alters the conformation of ERK1/2 which affects its phosphorylation, as evidenced by the decrease in ERK1/2 phosphorylation in DOX-treated cells and its inhibition by MnTBAP (Fig. 8).

In conclusion, our data provide evidence that superoxide is a key mediator of DOX-induced apoptosis through a mechanism that involves Bcl-2 downregulation and activation of the intrinsic death pathway. Superoxide mediates the down-regulation of Bcl-2 through ubiquitin-proteasomal degradation which is triggered by ERK1/2 inactivation. Such inactivation was shown to be associated with oxidative modification of the protein via Cys-SOH formation. This new finding may have important implications in the oxidative regulation of apoptosis regulatory proteins and in the etiology of chemotherapy-induced toxicities. It remains to be determined, however, whether such regulatory mechanisms occur *in vivo* and in other cell systems.

Acknowledgments

This work was supported by the National Institutes of Health Grant [R01-HL76340-04S1, R01-HL095579] (to Y.R.) and by the Thailand Research Fund Grant [RGJ-5.Q.CU/49/A.1] (to U.N.).

Abbreviations

DOX	doxorubicin
ROS	reactive oxygen species
zVAD-fmk	benzyloxy-carbonyl-Val-Ala-Asp-(OMe) fluoromethyl ketone
zIETD-fmk	benzyloxycarbonyl-Ile-Glu(OMe)-Thr-Asp(OMe)-fluoromethylketone
zLEHD-fmk	benzyloxycarbonyl-Leu-Glu(OMe)-His-Asp(OMe)-fluoromethylketone
control	CNTL
MnTBAP	Mn(III)tetrakis(4-benzoic acid) porphyrin chloride
CAT	cell permeable catalase, catalase-polyethylene glycol
DMTU	dimethylthiourea
MnSOD	manganese superoxide dismutase
H_2DCF-DA	dihydrodichlorofluorescein diacetate
DHE	dihydroethidium
ESR	electron spin resonance
DMPO	5,5-dimethyl-1-pyrroline-N-oxide
SDS-PAGE	sodium dodecyl sulfate-polyacrylamide gel electrophoresis
LAC	lactacystin

CMA	concanamycin A
Bcl-2-Ub	Bcl-2 ubiquitination
Cys-SOH	cysteine sulfenic acid

References

[1]. Singal PK, Iliskovic N, Li TM, Kumar D. Adriamycin cardiomyopathy: Pathophysiology and prevention. FASEB J. 1997; 11:931–6. [PubMed: 9337145]

[2]. Dorr RT, Alberts DS. Modulation of experimental doxorubicin skin toxicity by β-Adrenergic compounds. Cancer Res. 1981; 41:2428–32. [PubMed: 7237439]

[3]. Minotti G, Menna P, Salvatorelli E, Cairo G, Gianni L. Anthracyclines: molecular advances and pharmacologic developments in antitumor activity and cardiotoxicity. Pharmacol Rev. 2004; 56:185–229. [PubMed: 15169927]

[4]. To H, Ohdo S, Shin M, Uchimaru H, Yukawa E, Higuchi S, Fujimura A, Kobayashi E. Dosing time dependency of doxorubicin-induced cardiotoxicity and bone marrow toxicity in rats. J Pharm Pharmacol. 2003; 55:803–10. [PubMed: 12841941]

[5]. Wang J, Lu Z, Au JLS. Protection against chemotherapy-induced alopecia. Pharm Res. 2006; 23:2505–14. [PubMed: 16972183]

[6]. Roberts S, Khammo N, McDonnell G, Sewell GJ. Studies on the decontamination of surfaces exposed to cytotoxic drugs in chemotherapy workstations. J Oncol Pharm Pract. 2006; 12:95–104. [PubMed: 16984748]

[7]. Castiglia L, Miraglia N, Pieri M, Simonelli A, Basilicata P, Genovese G, Guadagni R, Acampora A, Sannolo N, Scafarto MV. Evaluation of occupational exposure to antiblastic drugs in an Italian hospital oncological department. J Occup Health. 2008; 50:48–56. [PubMed: 18285644]

[8]. Kalyanaraman B, Joseph J, Kalivendi S, Wang S, Konorev E, Kotamraju S. Doxorubicin-induced apoptosis: implications in cardiotoxicity. Mol Cell Biochem. 2002; 234-235:119–24. [PubMed: 12162424]

[9]. Liu LL, Li QX, Xia L, Li J, Shao L. Differential effects of dihydropyridine calcium antagonists on doxorubicin-induced nephrotoxicity in rats. Toxicol. 2006; 231:81–90.

[10]. Hancock JT, Desikan R, Neill SJ. Role of reactive oxygen species in cell signalling pathways. Biochem Soc Trans. 2001; 29:345–50. [PubMed: 11356180]

[11]. Fruehauf JP, Meyskens JL Jr. Reactive oxygen species: a breath of life or death? Clinical Cancer Res. 2007; 13:789–94. [PubMed: 17289868]

[12]. Li P, Nijhawan D, Budihardjo I, Srinivasula S, Ahmad M, Alnemri E, Wang X. Cytochrome c and dATP-dependent formation of Apaf-1/caspase-9 complex initiates an apoptotic protease cascade. Cell. 1997; 91:479–89. [PubMed: 9390557]

[13]. Korsmeyer SJ, Yin XM, Oltvai ZN, Veis-Novack DJ, Linette GP. Reactive oxygen species and the regulation of cell death by the Bcl-2 gene family. Biochim Biophys Acta. 1995; 1271:63–6. [PubMed: 7599227]

[14]. Gupta S. Molecular signaling in death receptor and mitochondrial pathways of apoptosis. Int J Oncol. 2003; 22:15–20. [PubMed: 12469180]

[15]. Tsang WP, Chau SPY, Kong SK, Fung KP, Kwok TT. Reactive oxygen species mediate doxorubicin induced p53-independent apoptosis. Life Sciences. 2003; 73:2047–58. [PubMed: 12899928]

[16]. Wang S, Konorev EA, Kotamraju S, Joseph J, Kalivendi S, Kalyanaraman B. Doxorubicin induces apoptosis in normal and tumor cells via distinctly different mechanisms. Intermediacy of H_2O_2 and p53-dependent pathways. J Biol Chem. 2004; 279:25535–43. [PubMed: 15054096]

[17]. Chen Y, Jungsuwadee P, Vore M, Butterfield DA, St Clair DK. Collateral damage in cancer chemotherapy: oxidative stress in nontargeted tissues. Mol Intervent. 2007; 7:147–56.

[18]. Cai J, Jones DP. Superoxide in apoptosis. Mitochondrial generation triggered by cytochrome c loss. J Biol Chem. 1997; 273:11401–4. [PubMed: 9565547]

[19]. Moungjaroen J, Nimmannit U, Callery PS, Wang L, Azad N, Lipipun V, Chanvorachote P, Rojanasakul Y. Reactive oxygen species mediate caspase activation and apoptosis induced by lipoic acid in human lung epithelial cancer cells through Bcl-2 downregulation. J Pharmacol Exp Ther. 2006; 319:1062–9. [PubMed: 16990509]

[20]. Azad N, Iyer AK, Manosroi A, Wang L, Rojanasakul Y. Superoxide-mediated proteasomal degradation of Bcl-2 determined cell susceptibility to chromium (VI)-induced apoptosis. Carcinogenesis. 2008; 29:1538–45. [PubMed: 18544562]

[21]. Wang L, Chanvorachote P, Toledo D, Stehlik C, Mercer RR, Castranova V, Rojanasakul Y. Peroxide is a key mediator of Bcl-2 down-regulation and apoptosis induction by cisplatin in human lung cancer cells. Mol Pharmacol. 2008; 73:119–27. [PubMed: 17911532]

[22]. Dimmeler S, Breitschopf K, Haendeler J, Zeiher AM. Dephosphorylationtargets Bcl-2 for ubiquitin-dependent degradation: a link between the apoptosome and the proteasome pathway. J Exp Med. 1999; 189:1815–22. [PubMed: 10359585]

[23]. Su B, Karin M. Mitogen-activated protein kinase cascades and regulation of gene expression. Curr Opin Immunol. 1996; 8:402–11. [PubMed: 8793994]

[24]. Ruvolo PP, Deng X, May WS. Phosphorylation of Bcl-2 and regulation of apoptosis. Leukemia. 2001; 15:515–22. [PubMed: 11368354]

[25]. Boukamp P, Petrussevska RT, Breitkreuz D, Hornung J, Markham A, Fusenig N. Normal keratinization in a spontaneously immortalized aneuploid human keratinocyte cell line. J. Cell Biol. 1988; 106:761–71. [PubMed: 2450098]

[26]. Inui S, Itami S, Pan HJ, Chang C. Lack of androgen receptor transcriptional activity in human keratinocytes. J Dermatol Sci. 2000; 23:87–92. [PubMed: 10808125]

[27]. Pessina ARA, Cerri A, Piccirillo M, Neri MG, Croera C, Fori P, Berti E. High sensitivity of human epidermal keratinocytes (HaCaT) to topoisomerase inhibitors. Cell Prolif. 2001; 34:243–52. [PubMed: 11529882]

[28]. Botchakarev VA. Molecular mechanisms of chemotherapy-induced hair loss. J Investig Dermatol Symp Proc. 8:72–5. 200.

[29]. Eidsmo L, Fluur C, Rethi B, Ygberg SE, Ruffin N, De Milito A, Akuffo H, Chiodi F. FasL and TRAIL induce epidermal apoptosis and skin ulceration upon exposure to Leishmania major. Am J Pathol. 2007; 170:227–39. [PubMed: 17200196]

[30]. Lecker SW, Goldberg AL, Mitch WE. Protein degradation by the ubiquitin-proteasomal pathway in normal and disease states. J Am Soc Nephrol. 2006; 17:1807–19. [PubMed: 16738015]

[31]. Breitschopf K, Haendeler J, Malchow P, Zeiher AM, Dimmeler S. Posttranslational modification of Bcl-2 facilitates its proteasome-dependent degradation: molecular characterization of the involved signaling pathway. Mol Cell Biol. 2000; 20:1886–96. [PubMed: 10669763]

[32]. Poole LB, Karplus PA, Claiborne A. Protein sulfenic acids in redox signaling. Annu Rev Pharmacol Toxicol. 2004; 44:325–47. [PubMed: 14744249]

[33]. Poole LB, Nelson KJ. Discovering mechanisms of signaling-mediated cysteine oxidation. Curr Opin Chem Biol. 2008; 12:18–24. [PubMed: 18282483]

[34]. Lemieux J, Maunsell E, Provencher L. Chemotherapy-induced alopecia and effects on quality of life among women with breast cancer: a literature review. Psycho-Oncology. 2008; 17:317–28. [PubMed: 17721909]

[35]. Trueb RM. Chemotherapy-induced alopecia. Semin Cutan Med Surg. 2009; 28:11–4. [PubMed: 19341937]

[36]. Gilleron M, Marachal X, Montaigne D, Franczak J, Neviere R, Lancel S. NADPH oxidases participate to doxorubicin-induced cardiac myocyte apoptosis. Biochem Biophys Res Commun. 2009; 388:727–31. [PubMed: 19699179]

[37]. Droge W. Free radicals in the physiological control of cell function. Physiol Rev. 2002; 82:47–95. [PubMed: 11773609]

[38]. Martin SS, Vuori K. Regulation of Bcl-2 proteins during anoikis and amorphosis. Biochim Biophys Acta. 2004; 1692:145–57. [PubMed: 15246684]

[39]. Hemann MT, Lowe SW. The p53–Bcl-2 connection. Cell Death Differ. 2006; 13:1256–9. [PubMed: 16710363]

[40]. Yeh PY, Chuang SE, Yeh KH, Song YC, Chang LLY, Cheng AL. Phosphorylation of p53 on Thr55 by ERK2 is necessary for doxorubicin-induced p53 activation and cell death. Oncogene. 2004; 23:3580–8. [PubMed: 15116093]

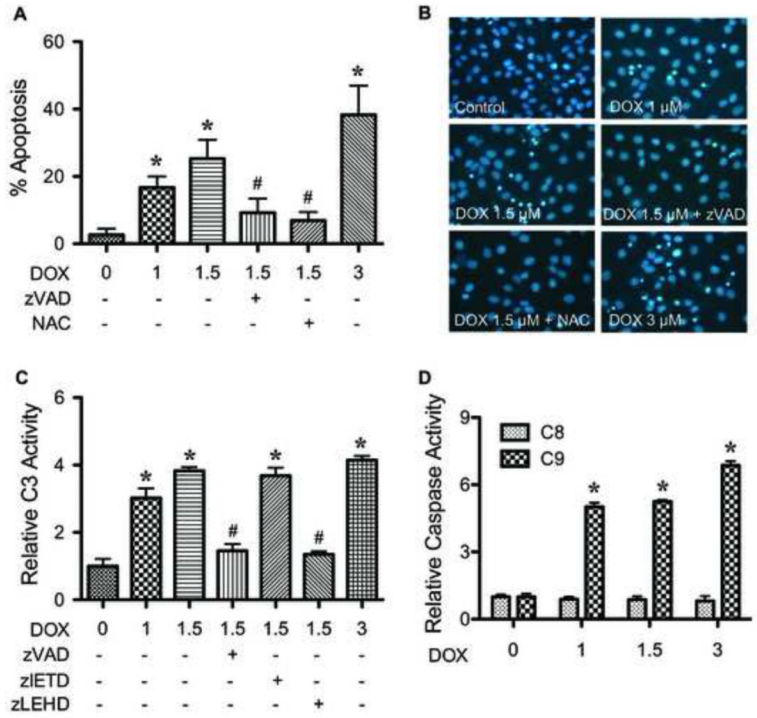

FIGURE 1.

Doxorubicin induces HaCaT cell apoptosis through mitochondrial death pathway. *A*, subconfluent monolayers (80%) of HaCaT cells were treated with various concentrations of DOX (0-3 μM) for 24 h in the presence or absence of pan-caspase inhibitor zVAD-fmk (10 μM) or *N*-acetyl cysteine (NAC) (2.5 mM) and analyzed for apoptosis by Hoechst 33342 assay. The presence of zVAD-fmk and NAC also had significant effects on the apoptotic signals induced by DOX at 1 and 3 μM (not shown). *B*, fluorescence micrographs of the treated cells stained with Hoechst dye. Apoptotic cells exhibited condensed and/or fragmented nuclei with bright nuclear fluorescence (original magnification, 400X). *C*, cells were similarly treated with DOX in the presence or absence of zVAD-fmk, caspase-8 inhibitor zIETD-fmk (10 μM), or caspase-9 inhibitor zLEHD-fmk (10 μM) and analyzed for caspase-3 activity using the fluorometric substrate FAM-DEVD-fmk. *D*, cells were treated with DOX (0-3 μM) and analyzed for caspase-8 and -9 activities using the fluorometric substrate FAM-LETD-fmk and FAM-LEHD-fmk, respectively. Plots are mean ± S.D. (n = 3). *, $p < 0.05$ versus non-treated control. #, $p < 0.05$ versus DOX-treated control (1.5 μM).

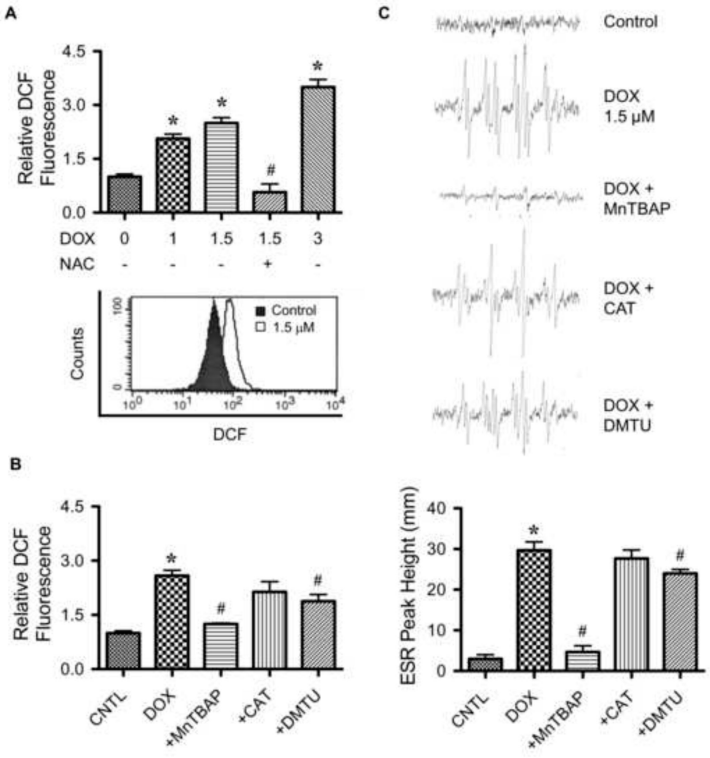

FIGURE 2.

Effect of doxorubicin on cellular ROS generation. *A*, HaCaT cells were treated with various concentrations of DOX (0-3 μM) in the presence or absence of *N*-acetyl cysteine (NAC) (2.5 mM) for 2 h, after which they were analyzed for ROS generation by flow cytometry using H_2DCF-DA as a fluorescent probe. Representative flow cytometric histograms are shown in the *lower* panel. *B*, cells were pretreated for 30 min with MnTBAP (50 μM), catalase (CAT, 7,500 units/ml), or DMTU (5 mM) followed by DOX treatment (1.5 μM) and analyzed for ROS generation at the maximum response time of 2 h by flow cytometry using H_2DCF-DA as a fluorescent probe. Increasing the dose of ROS scavengers had no further effect on the ROS generation (not shown). *C*, cells (1×10^6 cells/ml) were incubated in PBS containing the spin trapper DMPO (10 mM) with or without DOX (1.5 μM), MnTBAP (50 μM), catalase (CAT, 7,500 units/ml), and DMTU (5 mM). ESR spectra were recorded 5 min (peak response time) after the addition of the test agents. The spectrometer settings were as follows: receiver gain at 1.5×10^5, time constants at 0.3 sec, modulation amplitude at 1.0 G, scan time at 4 min, and magnetic field at 3,470 ± 100 G. Analysis of ESR measurements are shown in *lower* panel. Plots are mean ± S.D. (n = 3). *, $p < 0.05$ versus non-treated control. #, $p < 0.05$ versus DOX-treated control.

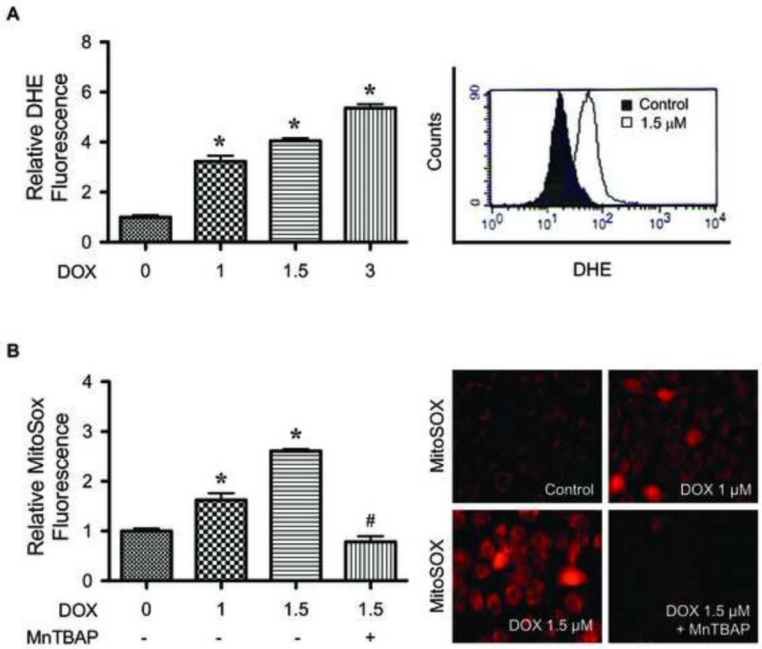

FIGURE 3.

Doxorubicin induces mitochondrial superoxide generation. *A*, HaCaT cells were treated with various concentrations of DOX (0-3 μM) for 2 h, after which they were analyzed for superoxide generation by flow cytometry using dihydroethidium (DHE) as a fluorescent probe. Representative flow cytometric histograms are shown in the *right* panel. *B*, cells were treated with DOX in the presence or absence of MnTBAP (50 μM) for 2 h, and analyzed for mitochondrial superoxide generation by fluorescence microscopy using MitoSOX™ Red as a probe. Representative micrographs demonstrating dose-dependent increase in mitochondrial MitoSOX™ fluorescence are shown in the *right* panel. Plots are mean ± S.D. (n = 3). *, $p < 0.05$ versus non-treated control.

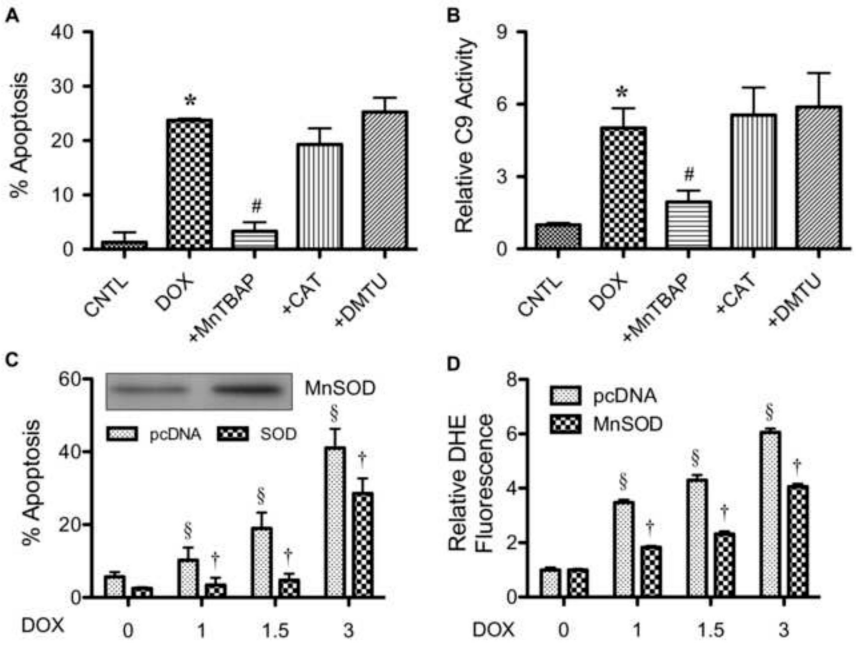

FIGURE 4.

Superoxide mediates doxorubicin-induced apoptosis. *A*, HaCaT cells were pretreated for 30 min with MnTBAP (50 μM), catalase (CAT, 7,500 units/ml), or DMTU (5 mM) followed by DOX treatment (1.5 μM) for 24 h and analyzed for apoptosis by Hoechst 33342 assay. *B*, cells were similarly treated with the ROS scavengers and DOX as described above and analyzed for caspase-9 activity using the fluorometric substrate FAM-LEHD-fmk. *C*, cells were transiently transfected with mitochondrial superoxide scavenging enzyme MnSOD or control pcDNA3 plasmid as described under *Material and Methods*. Transfected cells were treated with DOX (0-3 μM) for 24 h and analyzed for apoptosis by Hoechst 33342 assay. MnSOD expression of the transfected cells were analyzed by Western blotting. *D*, transfected cells were similarly treated with DOX and analyzed for superoxide generation by flow cytometry at 2 h after the treatment. Plots are mean ± S.D. (n = 3). *, $p < 0.05$ versus non-treated control. #, $p < 0.05$ versus DOX-treated control. §, $p < 0.05$ versus vector-transfected cells. †, $p < 0.05$ versus DOX-treated vector-transfected cells.

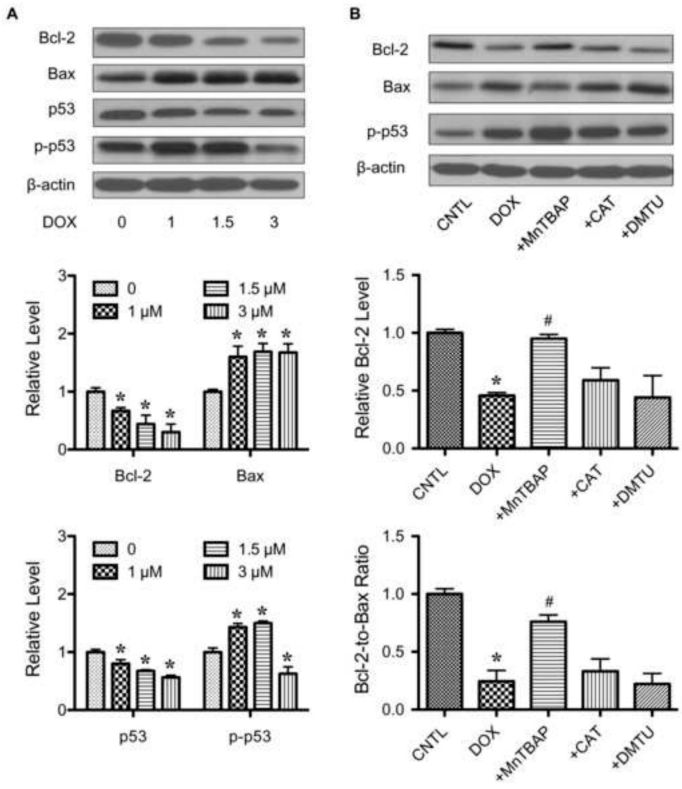

FIGURE 5.

Effect of doxorubicin and ROS scavengers on apoptosis regulatory proteins. *A*, HaCaT cells were treated with various concentration of DOX (0-3 μM) for 24 h. Cell lysates were prepared and analyzed for Bcl-2, Bax, p53 and phospho-p53 (p-p53) expression by Western blotting. Blots were reprobed with β-actin antibody to confirm equal loading of the samples. Immunoblot signals were quantified by densitometry and mean data from three independent experiments (one of which is shown here) was normalized to the result obtained in cells without treatment (control). *B*, cells were treated with DOX (1.5 μM) in the presence or absence of MnTBAP (50 μM), catalase (CAT, 7,500 units/ml), or DMTU (5 mM) and Bcl-2, Bax and p-p53 expression was determined. Plots are mean ± S.D. (n = 3). *, $p < 0.05$ versus non-treated control. #, $p < 0.05$ versus DOX-treated control.

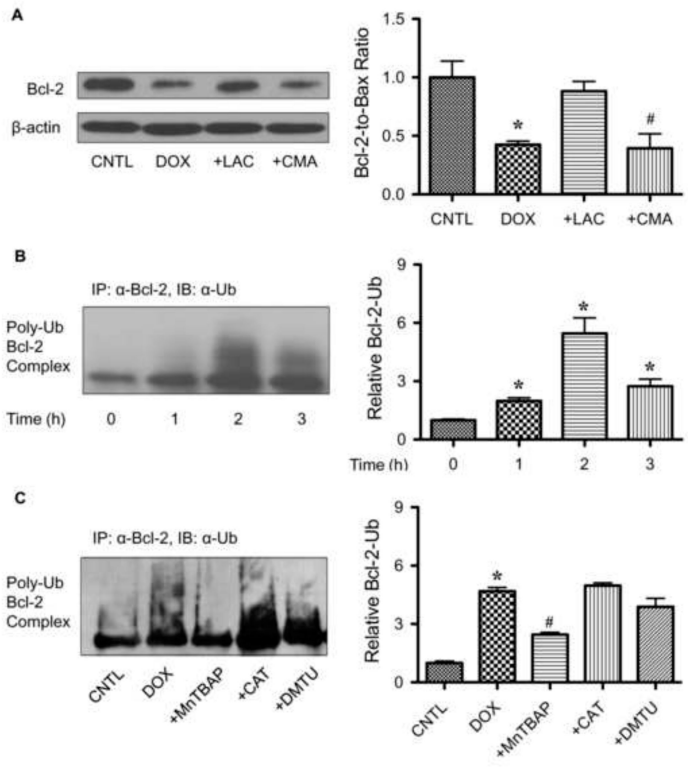

FIGURE 6.

Doxorubicin downregulates Bcl-2 through ubiquitin-proteasomal degradation. *A*, HaCaT cells were pretreated with the proteasome inhibitor lactacystin (LAC, 10 μM) or lysosome inhibitor concanamycin A (CMA, 1 μM) for 1 h, and then treated with DOX (1.5 μM) for 24 h. Bcl-2 expression was determined by Western blots using anti-Bcl-2 antibody. *B*, cells were pretreated with LAC (10 μM) for 1 h (to prevent proteasomal degradation of Bcl-2) and then treated with DOX (1.5 μM) for various times (0-3 h). Cell lysates were immunoprecipitated with anti-Bcl-2 antibody and the immune complexes were analyzed for ubiquitin by Western blotting. *C*, cells were pretreated with LAC (10 μM) for 1 h and then treated with DOX (1.5 μM) in the presence or absence of MnTBAP (50 μM), catalase (CAT, 7,500 units/ml), or DMTU (5 mM). Analysis of ubiquitin was performed as described at 2 h post-treatment where ubiquitination was found to be maximal. Plots are mean ± S.D. (n = 3). *, $p < 0.05$ versus non-treated control. #, $p < 0.05$ versus DOX-treated control.

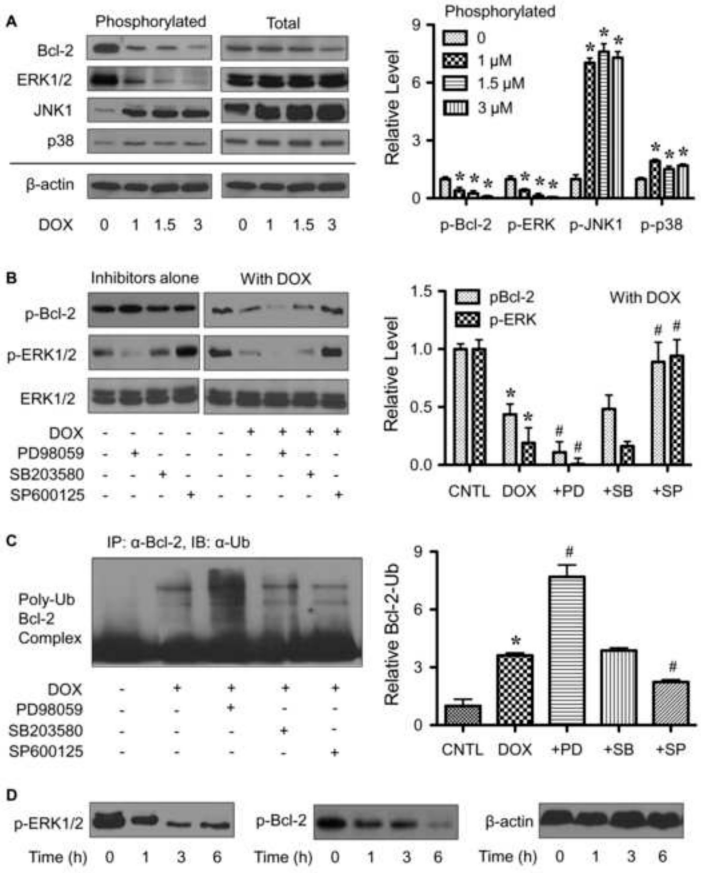

FIGURE 7.

Phosphorylation of Bcl-2 by ERK1/2 mediates Bcl-2 ubiquitination. *A*, HaCaT cells were treated with various concentrations of DOX (0-3 μM) for 6 h. Cell lysates were prepared and analyzed for phospho-Bcl-2 (p-Bcl-2, Ser 87) and various MAP kinases, including phosho-ERK1/2 (p-ERK1/2), phospho-JNKs (p-JNKs) and phospho-p38 kinase (p-p38) expression by Western blotting. Blots were reprobed with total Bcl-2, ERK1/2, JNKs, p38 and β-actin antibody to confirm equal loading of the samples. *B*, cells were treated with or without DOX (1.5 μM) in the presence or absence of PD98059 (ERK1/2 inhibitor, 25 μM), SB203580 (p38 inhibitor, 10 μM), and SP600125 (JNK inhibitor, 10 μM), and p-Bcl-2 and p-ERK1/2 were determined. Blots were reprobed with ERK1/2 antibody to confirm equal loading of the samples. *C*, cells were treated with DOX (1.5 μM) in the presence or absence of PD98059 (25 μM), SB203580 (10 μM), or SP600125 (10 μM). Analysis of Bcl-2 ubiquitination was performed as described at 2 h post-treatment where it was found to be maximal. *D*, cells were treated with DOX (1.5 μM) for various times (0-6 h) and p-Bcl-2 and p-ERK1/2 were determined. Plots are mean ± S.D. (n = 3). *, $p < 0.05$ versus non-treated control. #, $p < 0.05$ versus DOX-treated control.

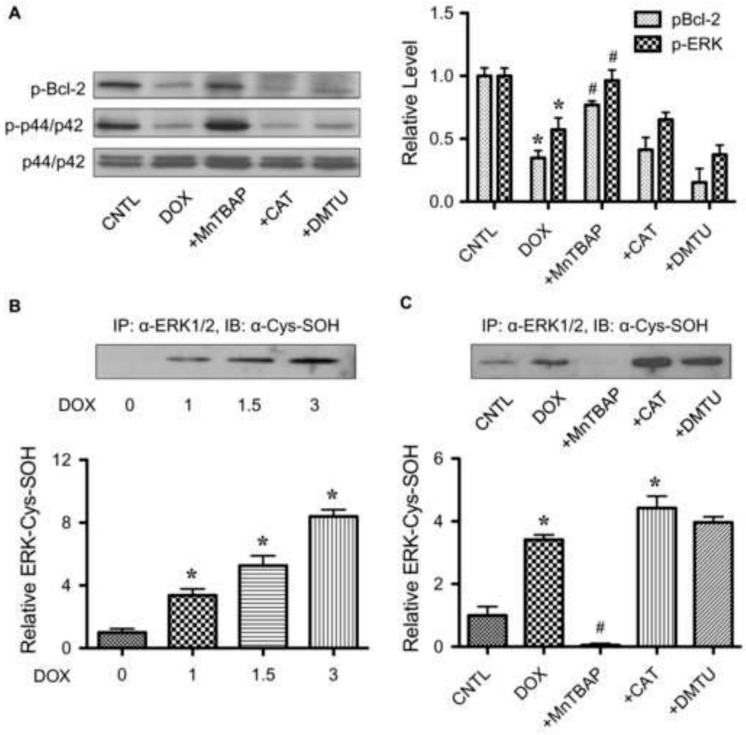

FIGURE 8.

Superoxide induces ERK1/2 inactivation and cysteine sulfenic acid formation. *A*, HaCaT cells were treated with DOX (1.5 μM) for 6 h in the presence or absence of MnTBAP (50 μM), catalase (CAT, 7,500 units/ml), or DMTU (5 mM), and phospho-Bcl-2 (p-Bcl-2) and phospho-ERK1/2 (p-ERK1/2) expression was determined by Western blotting. Blots were reprobed with ERK1/2 antibody to confirm equal loading of the samples. *B*, cells were treated with various concentration of DOX (0-3 μM) for 2 h and cell lysates were prepared and immunoprecipitated with anti-ERK1/2 (*lower*) antibody. The immune complexes were analyzed for cysteine sulfenic acid (Cys-SOH) by Western blotting. *C*, cells were treated with DOX (1.5 μM) in the presence or absence of MnTBAP (50 μM), catalase (CAT, 7,500 units/ml), or DMTU (5 mM). Analysis of ERK1/2 Cys-SOH was performed as described. Plots are mean ± S.D. (n = 3). *, $p < 0.05$ versus non-treated control. #, $p < 0.05$ versus DOX-treated control.